

EFFECT OF UNIAXIAL INITIAL STRESSES, PIEZOELECTRICITY AND THIRD ORDER ELASTIC CONSTANTS ON THE NEAR-SURFACE WAVES IN A STRATIFIED HALF-PLANE

I. Kurt^{1,*}, S. D. Akbarov^{1,2}, S. Sezer^{1,2}

ABSTRACT

Dispersion curves of a system consisting of a piezoelectric covering layer and metal half-plane under the uniaxial initial stresses perpendicular to the wave propagation direction are obtained within the scope of the Three-dimensional Linearized Theory of Elastic Waves in Initially Stressed Bodies. The elasticity relations of the metal half-plane material are described by the Murnaghan potential. The numerical results are discussed for PZT-2 covering layer and aluminum half-plane material. The influence of the initial stresses, the piezoelectricity of the covering layer, and the third order elastic constants on the near-surface wave propagation velocity is illustrated.

Keywords: *Uniaxial Initial Stress, Dispersion, Near-Surface Waves, Piezoelectric, Third Order Elastic Constants*

INTRODUCTION

Initial stresses can arise from the material thermal expansion, in the absence of applied loads (residual stress), and intentionally to improve the material performance or unintentionally from the manufacturing process. The effect of initial stresses on wave propagation in a piezoelectric stratified half-plane system is widely studied.

Propagation behavior of Love waves in a layered piezoelectric half-plane with initial stresses has been studied for electrically open and short cases. Results have shown the important effect of initial stress on the Love wave propagation and stress distribution [1]. Also same system model under the slowly varying inhomogeneous initial stresses has been studied to show the effect of initial stresses on dispersion curves of Love waves [2]. In a system consisting of an isotropic layer, a fiber-reinforced layer and isotropic half-plane under the influence gravity dispersion equation of Love waves have been investigated [3]. The combined effect of initial stress and finite deformation on the wave propagation velocity of Love waves at the boundary between a layer and a half-space is discussed [4]. According to the results, wave propagation velocity increases under the stretching stress and decreases under the compression stress with increasing dimensionless wavenumber kh .

Quasi-longitudinal waves under initial stresses in a system consisting of two facing half-planes have been investigated, and the results have shown that initial stresses cause a significant change in the velocity of surface waves [5]. The effect of initial stress on the reflection coefficients has been studied for an initially stressed piezoelectric half plane [6].

Torsional waves in a system consisting of a magneto-viscoelastic layer and an inhomogeneous half-plane with linear variation in rigidity and density have been investigated [7]. Furthermore, in a system consisting of an initially stressed inhomogeneous layer and an a linearly varying inhomogeneous half-space the propagation of torsional surface waves. According to this study the inhomogeneity of the constituents of the system and the initial stress affects the torsional wave propagation velocity considerably [8]. Torsional wave propagation velocity decreases with the increasing compressional initial stress and increasing with increasing dimensionless wavenumber kh .

However, these studies have not taken into consideration the third order elastic constants. Longitudinal wave propagation velocity in the two-layered circular hollow cylinder with the aluminum, steel and tungsten material layers has been studied under the uniaxial initial stretching and compression stress [9]. According to this study, the third order elastic constants of the materials affects considerably the axisymmetric wave propagation velocity.

This paper was recommended for publication in revised form by Regional Editor Tolga Taner

¹ *Department of Mechanical Engineering, Yildiz Technical University, Istanbul, Turkey*

² *Ins. Math. & Mech. Nat. Acad. Science of Azerbaijan, Baku*

**E-mail address: ikurt@yildiz.edu.tr*

Manuscript Received 16 June 2016, Accepted 4 November 2016

The influence of the third order elastic constants on near-surface wave propagation velocity has been shown in a metal elastic stratified half-plane [10]. Near-surface waves in metal half-plane covered with piezoelectric layer have been investigated, and the dispersion curves of the system have been obtained [11]. The effect of initial stresses along the wave propagation direction on the near surface wave dispersion curves considering the third order elastic constants for this system is studied [12]. For this system, results have been developed for different pairs of materials: PZT-2, PZT-4, PZT-6B for the covering layer; steel, aluminum for the half-plane in the electrically open and short cases [13]. In a PZT/Metal/PZT sandwich plate, Lamb waves have been investigated for the system both in the presence and absence of the initial stresses [14, 15].

In this study, a system consisting of a piezoelectric covering layer and a metal elastic half-plane under the uniaxial initial stresses perpendicular to the wave propagation direction is investigated. The effect of initial stresses, the piezoelectricity of the covering layer, and the third order elastic constants on near-surface wave propagation velocity for this system is evaluated.

MATHEMATICAL FORMULATION OF THE PROBLEM

The considered system consisting of a metal elastic half-plane covered by a piezoelectric layer with thickness h is subjected uniaxial initial stresses perpendicular to the interface between the constituents as shown in Figure 1. We associate the interface plane between the covering layer and half-plane with the Lagrangian coordinate system $Ox_1x_2x_3$ which in the natural state coincide with Cartesian coordinates. The piezoelectric covering layer and elastic half-plane occupy the domains $\{-\infty < x_1 < +\infty, 0, x_2, h, -\infty < x_3 < +\infty\}$ and $\{-\infty < x_1 < +\infty, -\infty, x_2, 0, -\infty < x_3 < +\infty\}$, respectively. Below, the upper indices (1) and (2) refer to the quantities concerning the covering layer and half-plane, respectively. The upper indices $(m), 0$ ($m = 1, 2$) refer to the quantities related to the initial stresses along the Ox_2 axis. Plane strain state is assumed in the Ox_1x_2 plane, and all sought quantities are independent from the x_3 coordinate.

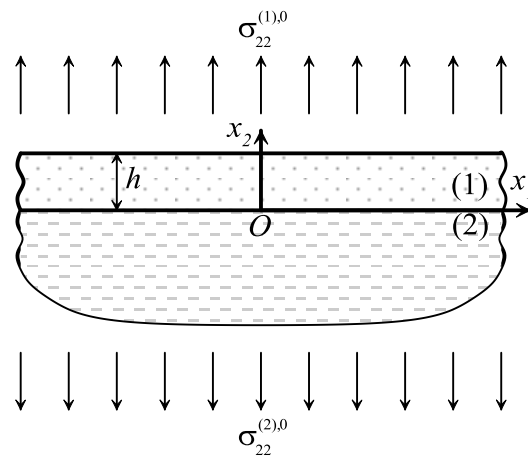


Figure 1. The geometry of the system consisting of a piezoelectric covering layer and a metal half-plane under uniaxial initial stress

The initial stresses in the covering layer and half-plane are defined within the framework of the classical linear theory of the electro-elasticity as follows:

$$\begin{aligned} \sigma_{22}^{(1),0} &= \text{const}_1 \neq 0, \sigma_{21}^{(1),0} = \sigma_{11}^{(1),0} = 0, \\ \sigma_{22}^{(2),0} &= \text{const}_2 \neq 0, \sigma_{21}^{(2),0} = \sigma_{11}^{(2),0} = 0. \end{aligned} \quad (1)$$

According to [16, 17], the equations of motion within the scope of classical linear theory of electro-elasticity are as follows:

$$\frac{\partial \sigma_{11}^{(m)}}{\partial x_1} + \frac{\partial \sigma_{12}^{(m)}}{\partial x_2} + \sigma_{22}^{(m),0} \frac{\partial^2 u_1^{(m)}}{\partial x_2^2} = \rho^{(m)} \frac{\partial^2 u_1^{(m)}}{\partial t^2},$$

$$\frac{\partial \sigma_{12}^{(m)}}{\partial x_1} + \frac{\partial \sigma_{22}^{(m)}}{\partial x_2} + \sigma_{22}^{(m),0} \frac{\partial^2 u_2^{(m)}}{\partial x_2^2} = \rho^{(m)} \frac{\partial^2 u_2^{(m)}}{\partial t^2},$$

$$\frac{\partial D_1^{(m)}}{\partial x_1} + \frac{\partial D_2^{(m)}}{\partial x_2} = 0, \quad (2)$$

where $\sigma_{ij}^{(m)}$, $u_i^{(m)}$, $D_i^{(m)}$, and $\rho^{(m)}$ are the components of the stress tensor, components of the displacement vector, components of the electrical displacement vector, and mass density of the m -th material, respectively.

The positive polarization direction of the piezoelectric material coincide with the Ox_2 axis. Constitutive equations of piezoelectric covering layer can be written as follows:

$$\sigma_{11}^{(1)} = c_{11}^{(1)} \frac{\partial u_1^{(1)}}{\partial x_1} + c_{13}^{(1)} \frac{\partial u_2^{(1)}}{\partial x_2} + e_{31}^{(1)} \frac{\partial \phi^{(1)}}{\partial x_2},$$

$$\sigma_{22}^{(1)} = c_{13}^{(1)} \frac{\partial u_1^{(1)}}{\partial x_1} + c_{33}^{(1)} \frac{\partial u_2^{(1)}}{\partial x_2} + e_{33}^{(1)} \frac{\partial \phi^{(1)}}{\partial x_2},$$

$$\sigma_{12}^{(1)} = c_{44}^{(1)} \left(\frac{\partial u_1^{(1)}}{\partial x_2} + \frac{\partial u_2^{(1)}}{\partial x_1} \right) + e_{15}^{(1)} \frac{\partial \phi^{(1)}}{\partial x_1},$$

$$D_1^{(1)} = e_{15}^{(1)} \left(\frac{\partial u_1^{(1)}}{\partial x_2} + \frac{\partial u_2^{(1)}}{\partial x_1} \right) - \epsilon_{11}^{(1)} \frac{\partial \phi^{(1)}}{\partial x_1},$$

$$D_2^{(1)} = e_{31}^{(1)} \frac{\partial u_1^{(1)}}{\partial x_1} + e_{33}^{(1)} \frac{\partial u_2^{(1)}}{\partial x_2} - \epsilon_{33}^{(1)} \frac{\partial \phi^{(1)}}{\partial x_2}, \quad (3)$$

where the $c_{ij}^{(1)}$, $e_{ij}^{(1)}$, $\epsilon_{ij}^{(1)}$, and $\phi^{(1)}$ are elasticity constants, piezoelectric constants, dielectric constants, and electric potential, respectively.

The material of the half-plane is non-linear pure elastic. Therefore, the motion of the half-plane can be described with the first and second equation in Eq. (2). The constitutive equations of the half-plane material are given by Murnaghan potential (Φ).

$$\Phi^{(2)} = \frac{1}{2} \lambda^{(2)} \left(A_1^{(2)} \right)^2 + \mu^{(2)} A_2^{(2)}$$

$$+ \frac{a^{(2)}}{3} \left(A_1^{(2)} \right)^3 + b^{(2)} A_1^{(2)} A_2^{(2)} + \frac{c^{(2)}}{3} A_3^{(2)}, \quad (4)$$

where $\lambda^{(2)}$ and $\mu^{(2)}$ are Lamé constants; $a^{(2)}$, $b^{(2)}$, and $c^{(2)}$ are the third order elasticity constants determined by ultrasonic methods; $A_1^{(2)}$, $A_2^{(2)}$, and $A_3^{(2)}$ are the first three invariants of the strain tensor and they are as follows:

$$A_1^{(2)} = \epsilon_{11}^{(2)} + \epsilon_{22}^{(2)},$$

$$A_2^{(2)} = \left(\epsilon_{11}^{(2)} \right)^2 + 2 \left(\epsilon_{12}^{(2)} \right)^2 + \left(\epsilon_{22}^{(2)} \right)^2,$$

$$A_3^{(2)} = \left(\epsilon_{11}^{(2)} \right)^3 + 3 \left(\epsilon_{12}^{(2)} \right)^2 \left(\epsilon_{11}^{(2)} + \epsilon_{22}^{(2)} \right) + \left(\epsilon_{22}^{(2)} \right)^3. \quad (5)$$

In Eq. (5), the components of the strain tensor are as follows:

$$\epsilon_{ij}^{(2)} = \frac{1}{2} \left(\frac{\partial u_i^{(2)}}{\partial x_j} + \frac{\partial u_j^{(2)}}{\partial x_i} + \frac{\partial u_n^{(2)}}{\partial x_j} \frac{\partial u_n^{(2)}}{\partial x_i} \right). \quad (6)$$

The components of the stress tensor can be defined as follows:

$$\sigma_{ij}^{(2)} = \frac{1}{2} \left(\frac{\partial}{\partial \varepsilon_{ij}^{(2)}} + \frac{\partial}{\partial \varepsilon_{ji}^{(2)}} \right) \Phi^{(2)}. \quad (7)$$

Linearizing the Eq. (7), the constitutive equations of the elastic half-plane can be written as follows:

$$\begin{aligned} \sigma_{11}^{(2)} &= A_{11}^{(2)} \varepsilon_{11}^{(2)} + A_{12}^{(2)} \varepsilon_{22}^{(2)}, \\ \sigma_{22}^{(2)} &= A_{12}^{(2)} \varepsilon_{11}^{(2)} + A_{22}^{(2)} \varepsilon_{22}^{(2)}, \\ \sigma_{12}^{(2)} &= 2\mu^{(2)} \varepsilon_{12}^{(2)} \end{aligned} \quad (8)$$

where

$$\begin{aligned} A_{11}^{(2)} &= \lambda^{(2)} + 2\mu^{(2)} \\ &+ \frac{2\sigma_{22}^{(2),0}}{3K_0^{(2)}} \left[(a^{(2)} + b^{(2)}) - (2b^{(2)} + c^{(2)}) \frac{\lambda^{(2)}}{2\mu^{(2)}} \right], \\ A_{22}^{(2)} &= \lambda^{(2)} + 2\mu^{(2)} + \frac{1}{\mu^{(2)}} (2b^{(2)} + c^{(2)}) \sigma_{22}^{(2),0} \\ &+ \frac{2\sigma_{22}^{(2),0}}{3K_0^{(2)}} \left[(a^{(2)} + b^{(2)}) - (2b^{(2)} + c^{(2)}) \frac{\lambda^{(2)}}{2\mu^{(2)}} \right], \\ A_{12}^{(2)} &= \lambda^{(2)} + \frac{b^{(2)}}{\mu^{(2)}} \sigma_{22}^{(2),0} + \frac{2\sigma_{22}^{(2),0}}{3K_0^{(2)}} \left[(a^{(2)} - b^{(2)}) \frac{\lambda^{(2)}}{\mu^{(2)}} \right], \\ \mu_{12}^{(2)} &= \mu^{(2)} + \frac{b^{(2)} \sigma_{22}^{(2),0}}{3K_0^{(2)}} + \frac{c^{(2)} \sigma_{22}^{(2),0}}{4\mu^{(2)}} + \frac{\lambda^{(2)} + 2\mu^{(2)}}{3K_0^{(2)}}, \\ K_0^{(2)} &= \lambda^{(2)} + \frac{2\mu^{(2)}}{3}, \\ \varepsilon_{ij}^{(2)} &= \frac{1}{2} \left(\frac{\partial u_i^{(2)}}{\partial x_j} + \frac{\partial u_j^{(2)}}{\partial x_i} \right), \end{aligned} \quad (9)$$

The complete contact conditions exist between the covering layer and half-plane ($x_2 = 0$) for the mechanical displacements and stresses as follows:

$$\begin{aligned} u_1^{(1)} \Big|_{x_2=0} &= u_1^{(2)} \Big|_{x_2=0}, \quad u_2^{(1)} \Big|_{x_2=0} = u_2^{(2)} \Big|_{x_2=0}, \\ \sigma_{12}^{(1)} \Big|_{x_2=0} &= \sigma_{12}^{(2)} \Big|_{x_2=0}, \quad \sigma_{22}^{(1)} \Big|_{x_2=0} = \sigma_{22}^{(2)} \Big|_{x_2=0}. \end{aligned} \quad (10)$$

The boundary condition for the electric potential is as follows:

$$\Phi^{(1)} \Big|_{x_2=0} = 0. \quad (11)$$

The boundary condition for the electric displacement is as follows:

$$D_2^{(1)} \Big|_{x_2=0} = 0. \quad (12)$$

The boundary conditions for the mechanical stresses on the top surface of the covering layer ($x_2 = h$) are as follows:

$$\sigma_{12}^{(1)} \Big|_{x_2=h} = 0, \quad \sigma_{22}^{(1)} \Big|_{x_2=h} = 0. \quad (13)$$

The boundary condition for the electric potential is as follows:

$$\phi^{(1)} \Big|_{x_2=h} = 0. \quad (14)$$

The boundary condition for the electric displacement is as follows:

$$D_2^{(1)} \Big|_{x_2=h} = 0. \quad (15)$$

The boundary conditions Eqs. (11) and (14) for the electrically shorted circuit, and the boundary conditions Eqs. (12) and (15) for the electrically open circuit should be satisfied.

The following decay conditions are satisfied for the near-surface waves in which there is no reflection of waves travelling along the negative x_2 direction in the half-plane.

$$\sigma_{ij}^{(2)} \rightarrow 0, u_i^{(2)} \rightarrow 0 \text{ as } x_2 \rightarrow -\infty, i, j = 1, 2 \quad (16)$$

METHOD OF SOLUTION

Substituting Eq. (3) into Eq. (2), the equations of electro-elastic motion of piezoelectric covering layer is obtained as follows:

$$\begin{aligned} c_{11}^{(1)} \frac{\partial^2 u_1^{(1)}}{\partial x_1^2} + (c_{44}^{(1)} + \sigma_{22}^{(1,0)}) \frac{\partial^2 u_1^{(1)}}{\partial x_2^2} + (c_{13}^{(1)} + c_{44}^{(1)}) \frac{\partial^2 u_2^{(1)}}{\partial x_1 \partial x_2} \\ + (e_{15}^{(1)} + e_{31}^{(1)}) \frac{\partial^2 \phi^{(1)}}{\partial x_1 \partial x_2} = \rho^{(1)} \frac{\partial^2 u_1^{(1)}}{\partial t^2}, \\ (c_{13}^{(1)} + c_{44}^{(1)}) \frac{\partial^2 u_1^{(1)}}{\partial x_1 \partial x_2} + c_{44}^{(1)} \frac{\partial^2 u_2^{(1)}}{\partial x_1^2} + (c_{33}^{(1)} + \sigma_{22}^{(1,0)}) \frac{\partial^2 u_2^{(1)}}{\partial x_2^2} \\ + e_{15}^{(1)} \frac{\partial^2 \phi^{(1)}}{\partial x_1^2} + e_{33}^{(1)} \frac{\partial^2 \phi^{(1)}}{\partial x_2^2} = \rho^{(1)} \frac{\partial^2 u_2^{(1)}}{\partial t^2}, \\ (e_{15}^{(1)} + e_{31}^{(1)}) \frac{\partial^2 u_1^{(1)}}{\partial x_1 \partial x_2} + e_{15}^{(1)} \frac{\partial^2 u_2^{(1)}}{\partial x_1^2} + e_{33}^{(1)} \frac{\partial^2 u_2^{(1)}}{\partial x_2^2} \\ - \varepsilon_{11}^{(1)} \frac{\partial^2 \phi^{(1)}}{\partial x_1^2} - \varepsilon_{33}^{(1)} \frac{\partial^2 \phi^{(1)}}{\partial x_2^2} = 0. \end{aligned} \quad (17)$$

Considering the harmonic wave propagation is in the Ox_1 axis direction, the displacements and electric potential of the covering layer can be represented as follows:

$$\begin{aligned} u_1^{(1)} &= A e^{bkx_2} \sin(kx_1 - \omega t), \\ u_2^{(1)} &= B e^{bkx_2} \cos(kx_1 - \omega t), \\ \phi^{(1)} &= C e^{bkx_2} \cos(kx_1 - \omega t). \end{aligned} \quad (18)$$

where A , B , and C are unknown constants, k is wave number, ω is angular frequency, and b is a parameter to be determined.

Substituting Eq. (18) into Eq. (17), we obtain the following equations to find the unknown constants A , B , and C in Eq. (18).

$$\begin{aligned} \left(c_{11}^{(1)} - (c_{44}^{(1)} + \sigma_{22}^{(1,0)}) b^2 - \rho^{(1)} \frac{\omega^2}{k^2} \right) A \\ + (c_{13}^{(1)} + c_{44}^{(1)}) b B + (e_{15}^{(1)} + e_{31}^{(1)}) b C = 0, \\ (c_{13}^{(1)} + c_{44}^{(1)}) b A - \left(c_{44}^{(1)} - (c_{33}^{(1)} + \sigma_{22}^{(1,0)}) b^2 - \rho^{(1)} \frac{\omega^2}{k^2} \right) B \\ - (e_{15}^{(1)} - e_{33}^{(1)} b^2) C = 0, \\ (e_{15}^{(1)} + e_{31}^{(1)}) b A - (e_{15}^{(1)} - e_{33}^{(1)} b^2) B \end{aligned}$$

$$-(\varepsilon_{33}^{(1)}b^2 - \varepsilon_{11}^{(1)})C = 0. \quad (19)$$

Taking the coefficient matrix of Eq. (19) as $[K]$, Eq. (19) can be rewritten as follows:

$$[K] \cdot \begin{Bmatrix} A \\ B \\ C \end{Bmatrix} = [K] \cdot \begin{Bmatrix} 1 \\ \alpha_1 \\ \alpha_\phi \end{Bmatrix} = 0 \quad (20)$$

In order to find a non-trivial solution of A , B , and C , following equation must be satisfied:

$$\det[K] = 0. \quad (21)$$

For a given value of $c = \omega/k$, there are six roots of b , and each root represents one component of wave modes propagating in the piezoelectric layer and yields a partial solution to the covering layer. Taking these roots as $b_n^{(1)}$ ($n=1,2,\dots,6$), displacements, electric potential and stresses of the covering layer can be rewritten as follows:

$$\begin{aligned} u_1^{(1)} &= \sum_{n=1}^6 A_n^{(1)} e^{b_n^{(1)}kx_2} \sin(kx_1 - \omega t), \\ u_2^{(1)} &= \sum_{n=1}^6 A_n^{(1)} \alpha_{1n}^{(1)} e^{b_n^{(1)}kx_2} \cos(kx_1 - \omega t), \\ \phi^{(1)} &= \sum_{n=1}^6 A_n^{(1)} \alpha_{\phi n}^{(1)} e^{b_n^{(1)}kx_2} \cos(kx_1 - \omega t), \\ \sigma_{ii}^{(1)} &= \sum_{n=1}^6 A_n^{(1)} \alpha_{iin}^{(1)} e^{b_n^{(1)}kx_2} \cos(kx_1 - \omega t), \quad i = 1, 2 \\ \sigma_{12}^{(1)} &= \sum_{n=1}^6 A_n^{(1)} \alpha_{12n}^{(1)} e^{b_n^{(1)}kx_2} \sin(kx_1 - \omega t). \end{aligned} \quad (22)$$

where $\alpha_{1n}^{(1)}$, $\alpha_{\phi n}^{(1)}$, and $\alpha_{ijn}^{(1)}$ are known constants and they can be obtained from Eq. (21) for the real roots of $b_n^{(1)}$, and some mathematical manipulations should be made for the complex roots of $b_n^{(1)}$ [11]. $A_n^{(1)}$ are six unknown constants used instead of the unknown constants A , B , and C in Eq. (18).

The displacements and stresses of the half-plane can be represented as follows:

$$\begin{aligned} u_1^{(2)} &= \varphi_1^{(2)}(x_2) \sin(kx_1 - \omega t), \\ u_2^{(2)} &= \varphi_2^{(2)}(x_2) \cos(kx_1 - \omega t). \end{aligned} \quad (23)$$

Substituting Eq. (8), (9), and (23) into Eq. (2), we obtain the following equations to find the functions $\varphi_1^{(2)}(x_2)$ and $\varphi_2^{(2)}(x_2)$ as in (26).

$$\begin{aligned} \frac{d^2 \varphi_1^{(2)}}{d(kx_2)^2} + b_{21} \varphi_1^{(2)} + c_{21} \frac{d\varphi_2^{(2)}}{d(kx_2)} &= 0, \\ \frac{d^2 \varphi_2^{(2)}}{d(kx_2)^2} + b_{22} \varphi_2^{(2)} + c_{22} \frac{d\varphi_1^{(2)}}{d(kx_2)} &= 0, \end{aligned} \quad (24)$$

where

$$b_{21} = -\frac{A_{11}^{(2)}}{\mu_{12}^{(2)} + \sigma_{22}^{(2),0}} + \frac{\rho^{(2)}\omega^2}{(\mu_{12}^{(2)} + \sigma_{22}^{(2),0})k^2},$$

$$\begin{aligned}
 c_{21} &= \frac{-A_{12}^{(2)} - \mu_{12}^{(2)}}{\mu_{12}^{(2)} + \sigma_{22}^{(2),0}}, \\
 b_{22} &= -\frac{\mu_{12}^{(2)}}{A_{22}^{(2)} + \sigma_{22}^{(2),0}} + \frac{\rho^{(2)} \omega^2}{(A_{22}^{(2)} + \sigma_{22}^{(2),0}) k^2} \\
 c_{22} &= \frac{A_{12}^{(2)} + \mu_{12}^{(2)}}{A_{22}^{(2)} + \sigma_{22}^{(2),0}}.
 \end{aligned} \tag{25}$$

Using Eq. (24), $\phi_1^{(2)}$ and $\phi_2^{(2)}$ can be obtained as follows:

$$\begin{aligned}
 \phi_1^{(2)}(x_2) &= Y_1^{(2)} e^{R_1^{(2)} k x_2} + Y_2^{(2)} e^{R_2^{(2)} k x_2}, \\
 \phi_2^{(2)}(x_2) &= Y_1^{(2)} \alpha_{11}^{(2)} e^{R_1^{(2)} k x_2} + Y_2^{(2)} \alpha_{12}^{(2)} e^{R_2^{(2)} k x_2}
 \end{aligned} \tag{26}$$

where

$$\begin{aligned}
 R_1^{(2)} &= \sqrt{-\frac{B_2}{2} + \sqrt{\left(\frac{B_2}{2}\right)^2 - C_2}}, \\
 R_2^{(2)} &= \sqrt{-\frac{B_2}{2} - \sqrt{\left(\frac{B_2}{2}\right)^2 - C_2}}, \\
 B_2 &= b_{21} + b_{22} - c_{21} c_{22}, \quad C_2 = b_{21} b_{22}.
 \end{aligned} \tag{27}$$

Substituting Eq. (26) into Eq. (23), and then Eq. (23) into Eq. (8), displacements and stresses of the half-plane can be rewritten as follows:

$$\begin{aligned}
 u_1^{(2)} &= \sum_{m=1}^2 Y_m^{(2)} e^{R_m^{(2)} k x_2} \sin(k x_1 - \omega t), \\
 u_2^{(1)} &= \sum_{m=1}^2 Y_m^{(2)} \alpha_{1m}^{(2)} e^{R_m^{(2)} k x_2} \cos(k x_1 - \omega t), \\
 \sigma_{ii}^{(2)} &= \sum_{m=1}^2 Y_m^{(2)} \alpha_{iim}^{(2)} e^{R_m^{(2)} k x_2} \cos(k x_1 - \omega t), \quad i = 1, 2 \\
 \sigma_{12}^{(2)} &= \sum_{m=1}^2 Y_m^{(2)} \alpha_{12m}^{(2)} e^{R_m^{(2)} k x_2} \sin(k x_1 - \omega t), \quad m = 1, 2.
 \end{aligned} \tag{28}$$

where $\alpha_{1m}^{(2)}$, $\alpha_{iim}^{(2)}$, and $\alpha_{12m}^{(2)}$ are known constants, and they can be obtained from Eqs. (24) and (26). $Y_m^{(2)}$ are two unknown constants.

Substituting the Eqs. (22) and (28) into the contact and boundary conditions Eqs. (10), (11), (13), and (14) or into the contact and boundary conditions Eqs. (10), (12), (13), and (15), system of homogeneous algebraic equations for the unknown constants $A_n^{(1)}$ ($n = 1, 2, \dots, 6$) and $Y_m^{(2)}$ ($m = 1, 2$) is obtained separately for the shorted and open circuit cases. By equating the determinant of the coefficient matrix of these equations to zero, we obtain the dispersion equation which can be presented formally as follows:

$$\begin{aligned}
 \Delta(c, kh, c_{11}^{(1)}, \dots, e_{31}^{(1)}, \dots, \epsilon_{11}^{(1)}, A_{11}^{(2)}, \\
 \dots, \mu_{12}^{(2)}, \sigma_{22}^{(1),0}, \sigma_{22}^{(2),0}) = 0.
 \end{aligned} \tag{29}$$

RESULTS AND DISCUSSION

Numerical solution of the dispersion equation Eq. (29) is made with bisection method for root finding using MATLAB in PC. In this method, for a given value of kh , roots of dispersion equation are found by changing wave phase velocity values $c = \omega/k$. In this study, the material of covering layer is PZT-2 and the material of half-plane is aluminum. The values of the mechanical, piezoelectrical, and dielectrical constants used in the numerical analyses are given in Table 1.

By taking the piezoelectric and dielectric constants of the piezoelectric material as zero, the covering layer turns into a transversal isotropic material without piezoelectricity. In Figure 2, first four lowest modes of the dispersion curves are obtained and plotted with dashed lines for the system which has a transversal isotropic covering layer. In this figure, solid lines represent the dispersion curves of the system which has a PZT-2 covering layer. Dispersion curves in Figure 2 are obtained for the case where piezoelectric layer is electrically shorted, and there are not initial stresses in the system. In Figure 2, $c_2^{(1)}$ is the transverse mode wave propagation velocity in the piezoelectric layer, and $c_2^{(1)} = \sqrt{(c_{44}^{(1)} + (e_{15}^{(1)})^2 / \epsilon_{11}^{(1)}) / \rho^{(1)}}$. In Figure 2, it is seen that the near-surface wave propagation velocity in the system with piezoelectric character is higher than in the system without piezoelectricity. Also in the higher values of kh , effect of piezoelectricity on wave propagation velocity is higher than in the lower values of kh . Same results in this figure is also available in [13], therefore it shows the accuracy of the PC algorithm.

Second, third and fourth dispersion curves for the system consisting of a PZT-4 covering layer and an aluminum metal elastic half-plane for the case where there are not initial stresses in the system are obtained in the paper [11]. These dispersion curves for the considered system are also obtained in [12] and [13] with the algorithm used in present investigation for the case where there are not initial stresses in the system. However, the first lowest mode dispersion curves for the system consisting of a PZT-4 covering layer and an aluminum metal elastic half-plane for the case where there are not initial stresses in the system are not given in the paper [11]. Present investigation and the study in [18] show that for the system consisting of a PZT-4 covering layer first lowest mode dispersion curves exist only before a certain value of the dimensionless wave number kh . Therefore, these results can be taken as validation of the testing of the algorithm used in the present investigation.

As the initial stresses on the covering layer and half-plane are equal ($\sigma_{22}^{(1),0} = \sigma_{22}^{(2),0} = P_0$), uniaxial initial stresses on the system can be given as follows:

$$\psi^{(1)} = P_0 / c_{44}^{(1)}. \quad (30)$$

In order to show the influence of the initial stresses on the near-surface wave propagation velocity, following notation will be used:

Table 1. Material Properties

Designation	Aluminum	PZT-2
$\rho (\times 10^3 \text{ kg} / \text{m}^3)$	2.70	7.60
$c_{11} (\times 10^{10} \text{ N} / \text{m}^2)$	10.20	13.50
$c_{33} (\times 10^{10} \text{ N} / \text{m}^2)$	10.20	11.30
$c_{44} (\times 10^{10} \text{ N} / \text{m}^2)$	2.60	2.22
$c_{13} (\times 10^{10} \text{ N} / \text{m}^2)$	5.0	6.81
$e_{15} (\text{C} / \text{m}^2)$	–	9.8
$e_{33} (\text{C} / \text{m}^2)$	–	9
$e_{31} (\text{C} / \text{m}^2)$	–	-1.9
$\epsilon_{11} (\times 10^{-9} \text{ F} / \text{m})$	–	8.7615
$\epsilon_{33} (\times 10^{-9} \text{ F} / \text{m})$	–	3.9825
$a (\times 10^5 \text{ MPa})$	3.08	–
$b (\times 10^5 \text{ MPa})$	-0.49	–
$c (\times 10^5 \text{ MPa})$	-2.92	–
$\lambda (\times 10^4 \text{ MPa})$	5.0	–
$\mu (\times 10^4 \text{ MPa})$	2.60	–

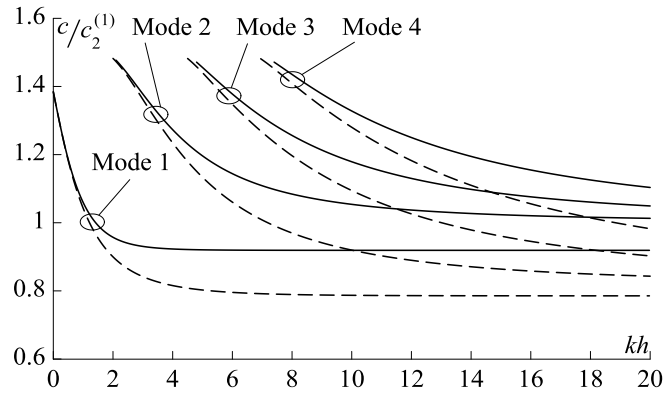


Figure 2. First four modes of dispersion curves

$$\eta = 10^3 \times (\bar{c} - c) / c \quad (31)$$

In Eq. (31), \bar{c} is the wave propagation velocity for the system with uniaxial initial stresses, and c is the wave propagation velocity for the system without initial stresses.

Figs. 3, 4, and 5 show the dependencies between the parameter η and kh for three different magnitude of the initial stretching and compression stresses ($\psi^{(1)} = 0.001, 0.002, 0.003$). In these figures, (a), (b), (c), and (d) show η and kh relation for the first, second, third, and fourth modes of the dispersion curves, respectively. This relation is shown with dashed lines for the system which has transversal isotropic covering layer and with solid lines for the system which has PZT-2 covering layer.

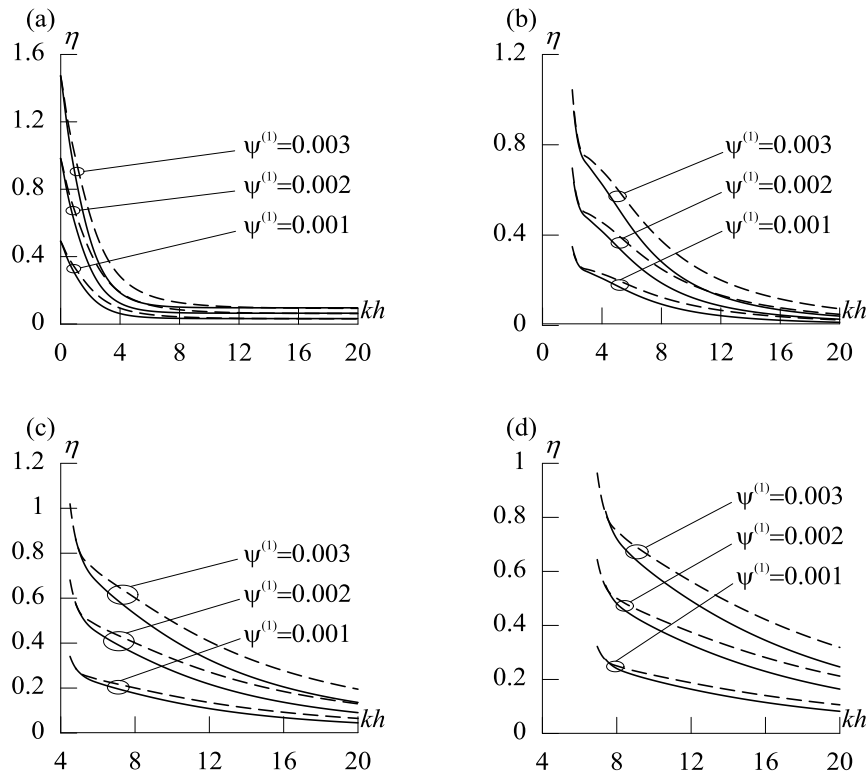


Figure 3. The effect of the uniaxial initial stretching on the near-surface wave propagation velocity in (a) first mode; (b) second mode; (c) third mode; (d) fourth mode

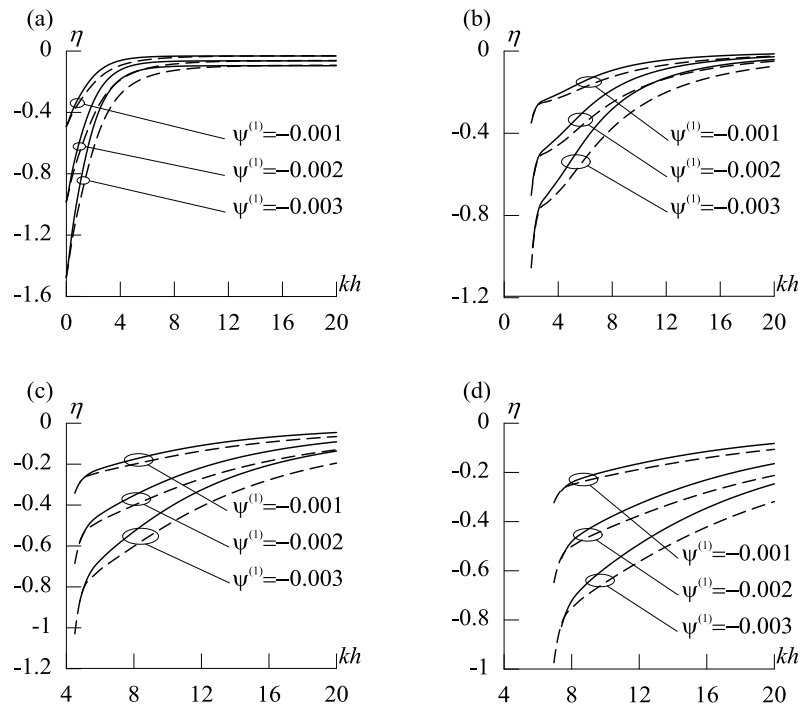


Figure 4. The effect of the uniaxial initial compression on the near-surface wave propagation velocity in (a) first mode; (b) second mode; (c) third mode; (d) fourth mode

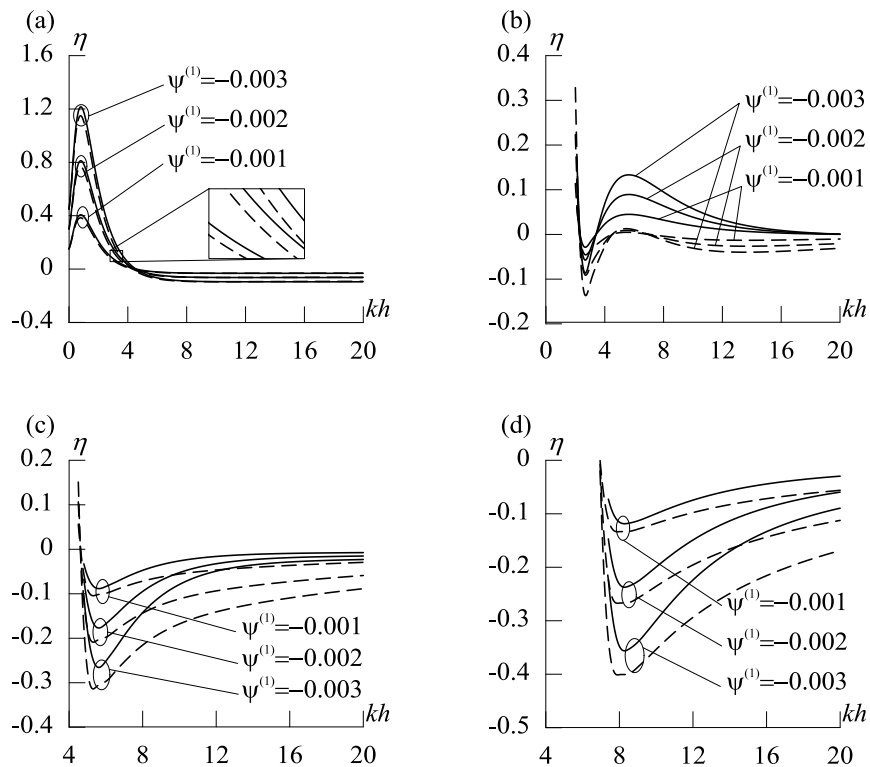


Figure 5. The effect of the uniaxial initial compression on the near-surface wave propagation velocity considering the third order elastic constants in (a) first mode; (b) second mode; (c) third mode; (d) fourth mode

Figure 3 shows the influence of the uniaxial initial stretching ($\psi^{(1)} > 0$) on the near-surface wave propagation velocity. In this figure, it is seen that the near-surface wave propagation velocity in the system under uniaxial initial stretching is higher than in the system without initial stresses. However, the piezoelectricity of the covering layer reduces the increment of wave propagation velocity.

Figure 4 shows the influence of the uniaxial initial compression ($\psi^{(1)} < 0$) on the near-surface wave propagation velocity. In this figure, it is seen that the near-surface wave propagation velocity in the system under uniaxial initial compression is lower than in the system without initial stresses. However, piezoelectricity of the covering layer reduces the decrease of wave propagation velocity.

Figs. 3 and 4 show that in the lower values of kh , effect of uniaxial initial stretching on wave propagation velocity is higher than in the higher values of kh . Also, this effect is significant in the first mode of the dispersion curves.

In Figure 3 and 4, third order elastic constants are not taken into account ($a^{(2)} = b^{(2)} = c^{(2)} = 0$). Figure 5 shows the influence of the uniaxial initial compression on the near-surface wave propagation velocity by taking third order elastic constant into consideration ($\psi^{(1)} < 0$, $a^{(2)}, b^{(2)}, c^{(2)} \neq 0$). In Figure 5, it is seen that third order elastic constants effect results significantly, especially in the lower values of kh .

CONCLUSION

Effects of the piezoelectricity of covering layer, third order elastic constants of the half-plane, and uniaxial initial compression and stretching, which is perpendicular to the wave propagation direction, on near-surface wave propagation velocity are investigated.

For concrete numerical investigations, the half-plane material is selected as aluminum and the covering layer material is selected as PZT-2. First four lowest modes of the dispersion curves are obtained for different cases in the system; without initial stresses (i), under uniaxial initial stretching (ii), under uniaxial initial compression without considering the third order elastic constant (iii), under uniaxial initial compression considering the third order elastic constant (iv). It is assumed that the positive polarization direction of the piezoelectric covering material coincide with the Ox_2 axis. Furthermore, the top and the bottom surfaces of the covering layer are electrically shorted.

According to the results, without the piezoelectric character of the covering layer, near-surface wave velocity is lower than in the system with piezoelectric character. Uniaxial initial stretching or compression significantly increases or reduces the near-surface wave propagation velocity. Also, the piezoelectricity of the covering layer affects the wave propagation velocity, considerably. Moreover, third order elastic constants have a remarkable effect on wave propagation velocity which increases or decreases depending on the values of kh .

NOMENCLATURE

h	piezoelectric covering layer thickness
$\sigma_{22}^{(m),0}$	initial stresses along the Ox_2 axis ($m = 1, 2$)
$\sigma_{ij}^{(m)}$	components of the stress tensor
$\varepsilon_{ij}^{(2)}$	components of the strain tensor
$u_i^{(m)}$	components of the displacement vector
$D_i^{(m)}$	components of the electrical displacement vector
$\rho^{(m)}$	mass density
$c_{ij}^{(1)}$	elasticity constants
$e_{ij}^{(1)}$	piezoelectric constants
$\varepsilon_{ij}^{(1)}$	dielectric constants
$\phi^{(1)}$	electric potential
Φ	Murnaghan potential

$\lambda^{(2)}, \mu^{(2)}$	Lamé constants;
$a^{(2)}, b^{(2)}, c^{(2)}$	the third order elasticity constants
$A_1^{(2)}, A_2^{(2)}, A_3^{(2)}$	first three invariants of the strain tensor
k	wave number
ω	angular frequency
c	wave propagation velocity without initial stress
\bar{c}	wave propagation velocity with initial stress
$c_2^{(1)}$	transverse mode wave propagation velocity of the layer
kh	dimensionless wavenumber

REFERENCES

- [1] Liu, H., Wang, Z. K., & Wang, T. J. (2001). Effect of initial stress on the propagation behavior of Love waves in a layered piezoelectric structure. *International Journal of Solids and Structures*, 38(1), 37-51.
- [2] Jin, F., Qian, Z., Wang, Z., & Kishimoto, K. (2005). Propagation behavior of Love waves in a piezoelectric layered structure with inhomogeneous initial stress. *Smart materials and structures*, 14(4), 515.
- [3] Kundu, S., Pandit, D. K., Gupta, S., & Manna, S. (2015). Love wave propagation in a fiber-reinforced medium sandwiched between an isotropic layer and gravitating half-space. *Journal of Engineering Mathematics*, 1-11.
- [4] Shams, M. (2016). Effect of initial stress on Love wave propagation at the boundary between a layer and a half-space. *Wave Motion*, 65, 92-104.
- [5] Abo-el-nour, N., & Alsheikh, F. A. (2009). Reflection and refraction of plane quasi-longitudinal waves at an interface of two piezoelectric media under initial stresses. *Archive of Applied Mechanics*, 79(9), 843-857.
- [6] Singh, B. (2010). Wave propagation in a prestressed piezoelectric half-space. *Acta mechanica*, 211(3-4), 337-344.
- [7] Kumari, P., Modi, C., & Sharma, V. K. (2016). Torsional waves in a magneto-viscoelastic layer over an inhomogeneous substratum. *The European Physical Journal Plus*, 131(8), 263.
- [8] Gupta, S., Ahmed, M., Manna, S., & Pramanik, A. (2015). Influence of Initial Stress and Inhomogeneity on Propagation of Torsional Type Surface Wave in a Crustal Layer. *International Journal of Geomechanics*, 06015012.
- [9] Akbarov, S. D. (2012). The influence of third order elastic constants on axisymmetric wave propagation velocity in the two-layered pre-stressed hollow cylinder. *Computers, Materials, & Continua*, 32(1), 29-60.
- [10] Akbarov, S. D., & Ozisik, M. (2003). The influence of the third order elastic constants to the generalized Rayleigh wave dispersion in a pre-stressed stratified half-plane. *International journal of engineering science*, 41(17), 2047-2061.
- [11] Jin, J., Wang, Q., & Quek, S. T. (2002). Lamb wave propagation in a metallic semi-infinite medium covered with piezoelectric layer. *International journal of solids and structures*, 39(9), 2547-2556.
- [12] Akbarov, S. D., Kurt, I., & Sezer, S. (2014, June). Dispersion of the near-surface waves in a system consisting of a pre-stressed piezoelectric covering layer and a pre-stressed metallic half-plane. In *Book of abstract of the XVIII conference mechanics of composite materials*, Riga, Latvia (Vol. 23, pp. 2-6).
- [13] Akbarov, S. (2015). *Dynamics of Pre-Strained Bi-Material Elastic Systems: Linearized Three-Dimensional Approach*. Springer.
- [14] Kurt, I., Akbarov, S. D., & Sezer, S. (2016). Lamb wave dispersion in a PZT/metal/PZT sandwich plate with imperfect interface. *Waves in Random and Complex Media*, 26(3), 301-327.
- [15] Kurt, I., Akbarov, S. D., & Sezer, S. (2016). The influence of the initial stresses on Lamb wave dispersion in pre-stressed PZT/Metal/PZT sandwich plates. *Structural Engineering and Mechanics*, 58(2), 347-378.
- [16] Guz, A.N., (2004). *Elastic Waves in Bodies with Initial (Residual) Stresses*. "ASK," Kiev.
- [17] Yang, J. (2004). *An introduction to the theory of piezoelectricity* (Vol. 9). Springer Science & Business Media.
- [18] Pang, Y., Liu, J. X., Wang, Y. S., & Zhao, X. F. (2008). Propagation of Rayleigh-type surface waves in a transversely isotropic piezoelectric layer on a piezomagnetic half-space. *Journal of Applied Physics*, 103(7), 074901.